

Parameters Involved in CVD Growth of CNT: A Review



Aunggat Shah, Gautam Saha, and Mrityunjoy Mahato

1 Introduction

Carbon is a light atom capable of forming single, double, and triple chemical bonds. CNTs were discovered by Ijima in 1991 [1] which have cylindrical structures, made by graphene sheets with sp^2 bonds open or closed ends [2, 3]. CNTs can be single-walled (diameter $\sim 2\text{--}3$ nm) and multi-walled (diameter $\sim 20\text{--}30$ nm). The length of CNT can be micrometer to centimeter range [4]. Based on the chiralities, CNTs can be of zig-zag, armchair, and chiral type. Zig-zag CNTs are hexagonal lattice and chiral CNTs have another pattern that may be semiconducting or semi-metallic. The lattice of armchair CNTs is rotated 90° with respect to the zig-zag pattern and possesses a metallic band structure [4]. The bandgap of CNTs may vary $0.18\text{--}1.8$ eV and, hence, can have tunable electrical properties [5]. CNTs are lightweight materials with high mechanical strength such as Young's moduli ~ 1 TPa (5 times than steel) and the tensile strength of 63 GPa (50 times than steel) [6]. CNTs are chemically inert and have good thermal conductivity ($\sim 2000\text{--}6000$ W/mK) [7, 8]. Due to the range of properties, CNTs have been applied in AFM or STM tips [9], microelectronics [10], electron field emission [11], energy storage [12], biosensors [13], composite materials [14], pharmaceutical [15], and solar cell [16]. However, CNT growth is a slow process and has a number of challenges for large-scale production. In this direction, quantification of the CNT growth process is important, and documenting the CNT growth parameters would be a valuable contribution.

A. Shah · M. Mahato (✉)

Physics Division, Department of Basic Sciences and Social Sciences, School of Technology, North-Eastern Hill University, Shillong, Meghalaya 793022, India
e-mail: mrityunjoyphy@gmail.com; mmahato@nehu.ac.in

G. Saha

Department of Information Technology, School of Technology, North-Eastern Hill University, Shillong, Meghalaya 793022, India

There are different methods to grow CNTs, such as arc discharge [17], laser ablation [18], electrolysis [19], polymer derived [20], and chemical vapor deposition (CVD) [21, 22]. Arc discharge method uses a high voltage through the graphite electrodes at high temperatures of 1700 °C and sub-atmospheric pressure. Some floating catalyst may be used, and the evaporated carbon from anode deposits on the cathode as CNTs [23]; however, the use of high temperature limits its scalability. Laser ablation uses a high-power laser with varying laser power, where a pure graphite is vaporized by laser with temperature of 1200 °C in an inert atmosphere [24]. The laser power is inversely proportional to the diameter of the SWCNTs [25]. Laser ablation suffers from scalability for industrial purpose. In CVD, a carbon source is passed through heated catalyst at temperatures 600–1100 °C under inert condition [21]. The nature of the hydrocarbons decides the types of CNTs, multi-walled or single-walled. CVD methods have been reported for large-scale productions of CNTs due to their economic viability and simplest reactor environment.

Recently, low temperature synthesis of CNTs has been tried where the carbon feedstocks are pretreated either at high temperature or by plasma. Mora et al [26] produced SWCNTs on Fe:Mo catalyst supported on Al₂O₃ powder at 300 °C by using plasma pretreated CH₄ gas. Nessim et al. [27] made preheating of incoming carbon source gasses at 770 °C to grow vertically aligned CNTs at 500 °C using Fe catalysts on Ta (Tantalum). Xiao et al. [28] demonstrated the growth of CNTs by PECVD using CH₄ gas at 450 °C over Ni–Al–Ni–layered catalysts (prepared by atomic layer deposition) over silicon wafer.

Despite plenty of literature on CNT growth, many components of the growth mechanisms in the CVD process are yet unknown [29–31]. Also, structural control of CNTs in terms of chirality, semiconducting/metallic ratio, and density of defects are still lacking in the CVD CNT growth process [32]. Allaedini et al. [4] reviewed the effect of various parameters and conditions of catalysts on the CNT production, such as catalyst size, shape, composition, concentration, and type of catalyst. However, some other parameters are also involved in the CNT production. In this review, we explore the effects of type of catalyst, temperature, nature of hydrocarbon feedstock, inert gas flow, and growth time on the yield and structural characteristics of CNTs. The experimentation on the variation of such parameters is still a challenge and such kinds of reproducible experimental data are poorly available in the literature. Thus, there is a great need in understanding the growth process and the parameters influencing the growth of CNTs by CVD route. In this review, effort is given to understand the effect of such parameters on CNT growth with the help of available literature.

2 Parameters in CVD Growth of CNTs

2.1 Effect of Catalyst

Catalysts play a critical role as the nucleation sites in CNT growth, and hence, a low cost, sustainable, and optimized catalyst is required for its optimum yield.

Metal, Metal oxide, and LDH Catalysts for CNT growth: Hussein et al. [33] reported the growth of MWCNTs using hexane gas over LDH catalysts (FeCoNiAl, CoNiAl, and FeNiAl), where CoNiAl catalyst gives a maximum yield of 183.5% with diameter of 20.60 nm. Nagaraju et al. [34] compared three catalysts, namely Co, Fe, and Co/Fe supported on alumina or silica, where alumina support giving better yield of MWCNTs at 700 °C. Seo et al. [35] compared Fe, Co, or Ni as the catalyst using acetylene carbon source at 720 °C with best yield found in Fe catalyst. Lee et al. [36] used thin film of Fe, Ni, and Co on silicon oxide substrate, where Ni resulted in best yield and Fe resulted in the best quality. In our earlier report, it was observed that NiO catalyst favors the growth of MWCNT [37, 38], whereas Fe₂O₃ and PbO favors the growth of amorphous carbon [39, 40].

Growth of CNTs on Porous Substrate/Catalyst: SWCNTs are often synthesized utilizing nanometer-sized particles as catalysts. However, Schneider et al. [41] prepared MWCNTs using other types of catalyst such as porous aluminum oxide at 900 °C using propylene as the carbon precursor.

Floating Catalysts for CNT Growth: Hussain et al. [42] used ferrocene as floating catalysts and ethylene as carbon source and produced SWCNTs of diameters 1.3–1.5 nm. Zhu et al. [43] pyrolyzed n-hexane (carbon source) in the presence of thiophene (sulfur source) where it was observed that the addition of sulfur favors SWCNTs. It has been reported that the addition of such compounds acts as a promoter for SWCNTs or DWCNTs [44] (Table 1).

2.2 Effect of Temperature

Growth temperature of CNTs is important for its crystallinity and the selectivity of catalysts. Mohammed et al. [46] observed carbon spheres in CVD reactions at temperatures below 650 °C. Thus, choosing the right temperature is critical for improving MWCNT selectivity and limiting the production of amorphous carbon and other types of carbon that may form as a result of side reactions. They used bimetallic Fe-Co catalysts supported on CaCO₃ to grow MWCNTs at 700 °C using acetylene as the carbon source with a yield of 170% in the temperature range of 700 °C to 750 °C. Bone and Coward [52] showed that acetylene undergoes polymerization at around 780 °C instead of forming CNTs. Liu et al. [47] prepared MWCNTs using PP plastic and HZSM-5 zeolite mixture over nickel catalyst and observed better graphitization at 800 °C than 750 °C with a lower yield. Venkatesan et al. [49] observed

Table 1 Summary of different parameters for CNT growth experimented in literature

Sl. No	Parameters	Optimized yield	Remarks	References
1	Effect of catalyst	183.5% (Catalyst + CNT)	Yields of different catalysts (FeCoNiAl, CoNiAl, FeNiAl), were 124.8, 183.5, and 110.5, respectively	[33]
		Fe was better than Co, Ni catalyst	CNT yields on metal catalysts with silica support were in the order Fe > Co > Ni	[35]
		Yield order: Ni > Co > Fe	CNT yields were better with Fe out of Ni, Fe, Co	[36]
		Floating Ferrocene catalyst	Ferrocene was used as the floating catalyst with ethylene as the carbon source to produce SWCNTs	[42]
		Floating Sulfur catalyst	It was observed that addition of sulfur in floating catalytic environment of ferrocene promoted the growth of SWCNTs	[43]
		On porous Al ₂ O ₃ (POAX) substrate	CNTs were grown on POAX substrate without the use of any catalysts	[41]
		Yield with catalyst thickness	Density of CNTs increased with larger catalyst thickness of 3 nm, 5 nm, and 7 nm	[45]
2	Effect of temperature	170% (Catalyst + CNT)	Yields of CNTs were 170% and 50% at 700 °C and 750 °C, respectively	[46]
		Yield of CNT growth from PP was optimized at 750 °C	Yields of CNTs were maximum at 750 °C in the temperature range (500 °C to 800 °C)	[47]
3	Effect of carbon source	Yield increased with smaller chain hydrocarbons	Yield of CNTs was better with methane out of various gasses (hexane, methane, naphthalene, benzene, anthracene, etc.) on Fe catalyst	[48]
4	Effect of growth time	170% (Catalyst + CNT)	Yields of CNTs were 170% and 156% at 60 min and 45 min, respectively	[46]

(continued)

Table 1 (continued)

Sl. No	Parameters	Optimized yield	Remarks	References
		Yield at 25 min	Yield with change in growth time (15, 25, and 35 min) showed CNT growth was best at 25 min	[49]
5	Effect of flow rate (carbon source)	170% (Catalyst + CNT) (acetylene)	Yields of CNTs achieved (at 700 °C and Ar flow of 230 ml/min) were 112% and 170% at acetylene flow of 150 ml/min and 190 ml/min, respectively	[47]
		185% (Catalyst + CNT) (methane)	Yield with flow rate of carbon (50 sccm) showed low defects CNT at 800 °C with a flow rate of 50 sccm	[50]
		Max yield at 100 sccm (ethylene)	Optimum yield at 100 sccm out of the experimented flow rate of 50, 75, 100, 125, and 150 sccm	[51]
		Max yield at 180 ml/min (acetylene)	Max yields at 180 ml/min among flow rates of 100, 140, 180 ml/min	[49]
	Effect of flow rate (inert gas)	170% (Catalyst + CNT)	Yields of CNTs were 170% and 134% at 230 ml/min and 290 ml/min of argon flow, respectively	[46]

the formation of amorphous carbon below 700 °C and above 1000 °C using NiO catalyst.

Li et al. [53] prepared CNTs at temperatures 500 °C, 600 °C, and 750 °C using Ni/NiO/Al₂O₄/Cu catalyst and methane carbon source. They observed CNTs above 720 °C and carbon fibers below 720 °C. Gulino et al. [54] produced MWCNTs at a large scale using Fe/Al₂O₃ catalyst and ethane as carbon precursor at 660 °C, while above 750 °C resulted in amorphous carbon. Zhou et al. [55] showed that sulfur is a growth promoter of CNTs at 1000 °C and yields of SWCNTs increases with increasing temperatures.

2.3 *Effect of Carbon Source*

The carbon precursor plays an important role in the growth of CNTs. The larger hydrocarbons are less stable, thus producing poor CNTs. However, smaller hydrocarbons are more stable and give higher quality CNTs.

Aliphatic Hydrocarbons as Carbon Source: Li et al. [48] used different hydrocarbons (methane, hexane, cyclohexane, benzene, anthracene, etc.) using Fe catalyst on MgO substrate for the growth of CNTs. The methane yielded to SWCNTs and cyclohexane/hexane produce MWCNTs. There must be a correlation between the molecular weight of carbon source and CNT growth; however, still it is not yet quantified. Shah et al. [50] reported yield of MWCNTs of 185% at 800 °C on Pt-W catalysts using methane as the carbon source.

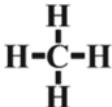

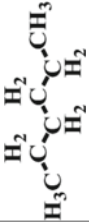
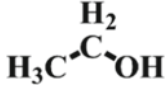

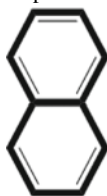
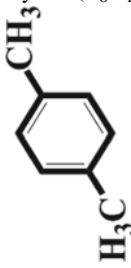
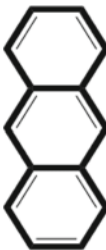

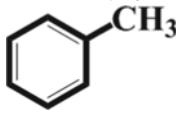
Aromatic Hydrocarbons as Carbon Source: Li et al. [56] experimented on different aromatic hydrocarbons like benzene, naphthalene, and anthracene and observed that smaller aromatic compounds (benzene) favor the growth of SWCNTs. Das et al. [57] used aromatic hydrocarbons: benzene, toluene, xylene, and trimethyl benzene using ferrocene as the catalyst, where toluene resulted in CNT yield 30.5% with 96% purity. Therefore, it can be concluded that aromatic hydrocarbons and methane favor SWCNTs, cyclic hydrocarbons (cyclohexane) favor MWCNTs, and linear chained hydrocarbons (hexane) favor carbon fibers.

Pyrolyzed Hydrocarbons from Plastics as Carbon Source: Plastics can also be used for the preparation of CNTs by the process of pyrolysis and subsequent deposition of the pyrolyzed hydrocarbons on the catalytic bed. This process is usually conducted in a two or three stage pyrolysis reactor. Demirba [58] showed that there is a decrease in chain length from C₂–C₈ to C₂–C₆ with an increase in pyrolysis temperature (650–875 °C) for PS (polystyrene). Encinar and Gonzalez [59] pyrolyzed plastic wastes at 800 °C which breaks down to smaller hydrocarbons of chain length C₁–C₃. Wu et al. [60] analyzed the pyrolyzed products of waste plastics at 500 °C and found the hydrocarbon chain length to be C₁–C₄. Thus, it is concluded that with an increase in pyrolysis temperature of plastics there is a decrease in the length of the hydrocarbons produced which consequently leads to a better formation of CNTs (Table 2).

2.4 *Effect of Growth Time*

Growth time plays an important role in the morphology of the CNTs produced during the CVD process. CNT formation takes place within just a few minutes of the growth process. The shorter reaction time favors the growth of CNTs with smaller diameters and longer growth times favor the growth of CNTs with longer diameters. However, Mohammed et al. 2017 [46] reported an increase in CNT yield with the increase in growth time from 45 to 60 min at 700 °C and also observed a decrease in CNT yield at 750 °C. Venkatesan et al. [49] showed that the optimum growth time is between 20

Table 2 Molecular structure of hydrocarbons used in CNT growth as carbon source (drawn using ChemDraw software)

<i>Aliphatic hydrocarbon source</i>			
Methane (CH ₄) 	Acetylene (C ₂ H ₂) HC≡CH	Ethane (C ₂ H ₄) H₃C-CH₃	Butylene (C ₄ H ₈) 
Hexane (C ₆ H ₁₄) 	Ethanol (C ₂ H ₅ OH) 	Ethylene (C ₂ H ₄) H₂C=CH₂	Carbon Monoxide (CO) ⁺O≡C⁻
<i>Aromatic hydrocarbon source</i>			
Benzene (C ₆ H ₆) 	Naphthalene (C ₁₀ H ₈) 	Xylene (C ₈ H ₁₀) 	Anthracene (C ₁₄ H ₁₀) 
Cyclohexane (C ₆ H ₁₂) 	Toluene (C ₇ H ₈) 	-	-

and 27 min while below 15 min and above 35 min lead to the formation of amorphous carbon and defective structures.

2.5 Effect of Flow Rate of Inert Gas and Carbon Source

Mohammed et al. [46] studied the effects of argon gas flow rate (230–290 ml/min) and hydrocarbon gas flow rate (150–190 ml/min). They observed that the yield of CNTs increased with an increase in acetylene flow but no change due to argon flow rate. Shukrullah et al. [51] experimented on ethylene flow rates from 50 to 100 sccm, where the optimum flow rate of 100 sccm led to the formation of well-structured

CNTs and above which the product showed structural defects. Venkatesan et al. [49] experimented on precursor gas flow rate (100–180 ml/min), where tubular structures formed above 180 ml/min and no graphitization below 100 ml/min.

2.6 Reactor Type and Size

Mullite versus Alumina Reactor Tube: Rodiles et al. [61] experimented on mullite ($\text{Al}_{4+2x}\text{Si}_{2-2x}\text{O}_{10-x}$ ($x \approx 0.4$)) and alumina (Al_2O_3) reactor type and observed the higher catalytic activity of mullite over alumina.

Hot Wall versus Cold Wall Reactor: CVD reactors can also be categorized by the temperature of the reactor wall, namely hot-wall CVD and cold-wall CVD. In hot-wall CVD, the entire reactor tube is maintained at the same temperature and is preferred for exothermic reactions. In contrast, cold-wall CVD employs heating of only the substrate within the reactor chamber by using RF induction or radiation lamps, while the walls of the reactor remain cold. The advantage of hot-wall CVD is the temperature uniformity across the entire reactor and possesses higher reaction volume; hence, it is more likely to be scaled up for better yield. Cold wall CVD is most useful for in situ analysis and experimentation [62].

2.7 Modeling and Optimizing of Different Parameters

There is very rare literature available which is dealing with the optimization and modeling of CNT growth using all possible parameters involved. However, some literature attempted to optimize a few parameters within a limited scope. Masouleh et al. [64] attempted to model the CNT growth using ferrocene as the floating catalyst and xylene as carbon source. They used a reactor reported by Maghrebi et al. [63] and assumed the decomposition of ferrocene to be a single-step process as shown in Eq. 1 (Fig. 1):

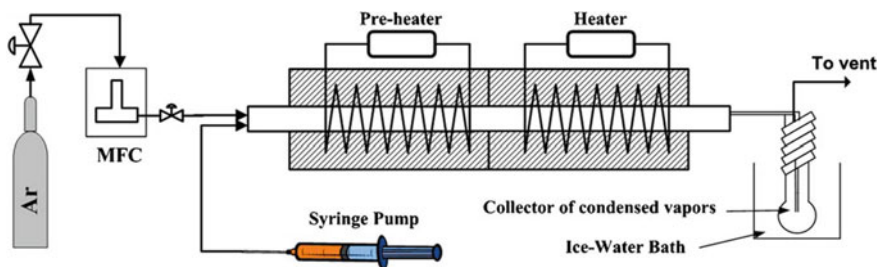
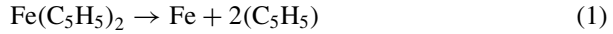


Fig. 1 The schematic diagram of CNT growth apparatus (Reproduced with prior permission from Maghrebi et al. [63])



The rate of decomposition of ferrocene is given by [64]:

$$-rA = 1.0 \times 10^{14} [\text{s}^{-1}] \exp\left(\frac{-209[\frac{\text{kJ}}{\text{mol}}]}{RT}\right) C_{\text{fer}} \quad (2)$$

Hence, the mass balance equation for ferrocene decomposed in the reactor is given by [64]:

$$-kC_{\text{fer}} = U_r \nabla_z C_{\text{fer}} \quad (3)$$

The mass balance equation of iron production ferrocene is given by [64]:

$$kC_{\text{fe}} - \frac{4K_c D_{\text{in}} C_{\text{fe}}}{D_{\text{out}}^2 - D_{\text{in}}^2} = U_r \nabla_z C_{\text{fer}} \quad (4)$$

Xylene undergoes thermal decomposition into toluene, benzene, methane, and C2 hydrocarbons. However, Masouleh et al. assumed the conversion of xylene to CNTs as a one-step reaction as follows [64]:

$$-(k'_A + k'_{\text{CNT}})C_X = U_r \nabla_z C_x \quad (5)$$

The amount of iron particles formed in the reactor directly affects the formation of CNTs as these iron particles act as nucleation sites for the growth of CNTs. The amount of iron nanoparticles formed is given by [64]:

$$\Theta = M_{\text{fe}} K_C C_{\text{fe}} \frac{D_{\text{out}}^2 - D_{\text{in}}^2}{4(D_{\text{out}} + D_{\text{in}})L} t \quad (6)$$

They observed that an increase in ferrocene concentration leads to an increase in the amount of iron produced which in turns increases CNT production following Eq. 7 [64]:

$$k'_{\text{CNT}} = k_{0\text{CNT}} \frac{4(D_{\text{out}} + D_{\text{in}})}{D_{\text{out}}^2 - D_{\text{in}}^2} \Theta \exp\left(\frac{-E_{\text{CNT}}}{RT}\right) \quad (7)$$

It was found that higher concentration of xylene and ferrocene leads to larger CNTs. Though, there is a 20% difference in the model prediction and the experimental value. They also observed that the maximum CNT heights were attained in the temperature range of 825–875 °C [64].

Where C_i = component (i) molar concentration (mol/m³); D_{in} = substrate diameter (m); D_{out} = quartz reactor diameter (m); k_{0A} = pre-exponential factor for the

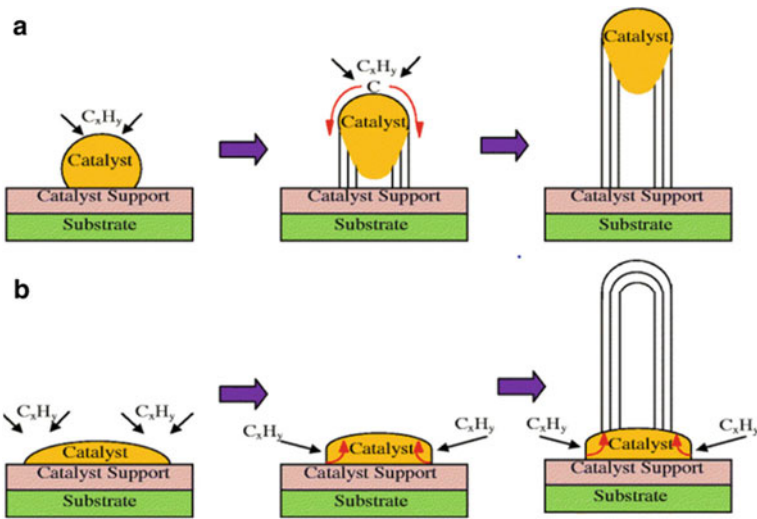


Fig. 2 Tip growth (a) and base growth (b) mechanisms of CNT (Reproduced with prior permission from Venkataraman et al. [65])

formation of amorphous carbon (m/s); $k_{0\text{CNT}}$ = pre-exponential factor for the formation of graphitic carbon (m^3/g of Fe); k'_{CNT} = rate constant of CNT formation (1/s); t = time (s); U_r = feedstock velocity (m/s); θ = weight by surface area of Fe (g/m^2); r_A = ferrocene decomposition rate; and M_{Fe} = molecular weight Fe (56 kg/kmol).

Tip growth and base growth mechanism: The hydrocarbon vapor decomposes into carbon and hydrogen when it touches metal or catalyst and subsequently hydrogen gas evaporates. Tip growth or base growth model for CNT growth depends upon the type of catalyst–substrate interaction. Tip growth of CNT occurs by the poor interaction of the hydrocarbon with metal catalyst due to the low concentration of metal. The base growth of CNT is facilitated by the strong interaction of hydrocarbon vapor with the catalyst, due to the higher concentration of metal available in the reaction [65]. Gohier et al. [66] reported a base growth model of CNT with smaller structures like SWCNTs or FWCNTs. However, they observed that the growth model switches from tip growth to base growth with decreasing particle size of the catalyst (Fig. 2).

3 Conclusion

In this work, we have reviewed the effects of various reaction parameters for the growth of CNTs. The optimum and best conditions of the reaction parameters have been described. The transition metal-based catalysts were found to be the better catalysts for CNT growth alongside porous substrates. The optimum growth temperature

range is found to be 700–750 °C; however, the growth temperature for SWCNTs is around 1000 °C. It is found in many experiments that ferrocene plays an important role as floating catalysts alone or along with other catalysts. It is also to be noted that many experiments use sulfur-based compounds, which act as promoters for SWCNT growth. It is found from the literature that the long-chain aliphatic hydrocarbons favor the growth of MWCNTs and a stable carbon compound like aromatic hydrocarbons favor the growth of SWCNT. A moderate growth time (maybe 25–35 min) can be an optimized growth time for better graphitization of CNTs. Optimization of growth parameters with different reactor types is still a less studied topic and needs attention in future work. Future work may involve theoretical and modeling work to understand the underlying mechanism of CNT growth, along with extensive experimentation with the growth parameters to complement the modeling work.

Acknowledgements Authors would like to acknowledge DST-SERB, Government of India, for financial support through SERB project (No. EMR/2016/004219) sanctioned to Dr. Mrityunjay Mahato.

References

1. Iijima S (1991) Helical microstructures of graphitic carbon. *Nature* 354:56–58
2. De Volder MFL, Tawfick SH, Baughman RH, Hart AJ (2013) Carbon nanotubes: present and future commercial applications. *Science* 339:535–539
3. Eatemadi A, Daraee H, Karimkhanloo H, Kouhi M, Zarghami N, Akbarzadeh A, Abasi M, Hanifehpour Y, Joo SW (2014) Carbon nanotubes: properties, synthesis, purification, and medical applications. *Nanoscale Res Lett* 9:393–406
4. Allaedini G, Tasirin SM, Aminayi P, Yaakob Z, MeorTalib MZ (2016) Carbon nanotubes via different catalysts and the important factors that affect their production: a review on catalyst preferences. *Int J Nano Dimens* 7:186–200
5. Elliott JA, Sandler JKW, Windle AH, Young RJ, Shaffer MSP (2004) Collapse of single-walled carbon nanotubes is diameter dependent. *Phys Rev Lett* 92(9):1–4
6. Saifuddin N, Raziah AZ, Junizah AR (2013) Carbon nanotubes: a review on structure and their interaction with proteins. *J Chem* 2013:1–18
7. Yu MF, Files BS, Arepalli S, Ruoff RS (2000) Tensile loading of ropes of single wall carbon nanotubes and their mechanical properties. *Phys Rev Lett* 84:5552–5555
8. Hana Z, Fina A (2011) Thermal conductivity of carbon nanotubes and their polymer nanocomposites: a review. *Prog Polym Sci* 36:914–944
9. Baughman RH, Zakhidov AA, Heer WA (2002) Carbon nanotubes: the route toward applications. *Science* 297:787–792
10. Ionescu AM, Riel H (2011) Tunnel field-effect transistors as energy-efficient electronic switches. *Nature* 479:329–337
11. Riggs JE, Guo Z, Carroll DL, Sun Y-P (2000) Strong luminescence of solubilized carbon nanotubes. *J Am Chem Soc* 122:5879–5880
12. Dai L, Chang DW, Baek JB, Lu W (2012) Carbon nanomaterials for advanced energy conversion and storage. *Small* 8:1130–1166
13. Köhler AR, Som C, Helland A, Gottschalk F (2008) Studying the potential release of carbon nanotubes throughout the application life cycle. *J Cleaner Prod* 16:927–937
14. Gojny F, Wichmann M, Köpke U, Fiedler B, Schulte K (2004) Carbon nanotube-reinforced epoxy-composites: enhanced stiffness and fracture toughness at low nanotube content. *Compos Sci Technol* 64:2363–2371

15. He H, Pham-Huy LA, Dramou P, Xiao D, Zuo P, Pham-Huy C (2013) Carbon nanotubes: applications in pharmacy and medicine. *BioMed Res Int* 4:145–156
16. Mahmood SS, Atiya AJ, Abdulrazzak FH, Alkaim AF, Hussein FH (2021) A review on applications of Carbon Nanotubes (CNTs) in solar cells. *J Med Chem Sci* 4:225–229
17. Mroz P, Tegos GP, Gali H, Wharton T, Sarna T, Hamblin MR (2008) Fullerenes as photosensitizers in photodynamic therapy. *Med Chem Pharmacol Potential Fullerenes Carbon Nanotubes* :79–106
18. Hu J, Odom TW, Lieber CM (1999) Chemistry and physics in one dimension: synthesis and properties of nanowires and nanotubes. *Acc Chem Res* 32:435–445
19. Iyer VS, Vollhardt KPC, Wilhelm R (2003) Near-quantitative solid-state synthesis of carbon nanotubes from homogeneous diphenylethyne-cobalt and–Nickel complexes. *Angew Chem* 115:4515–4519
20. Cho WS, Hamada E, Kondo Y, Takayanagi K (1996) Synthesis of carbon nanotubes from bulk polymers. *Appl Phys Lett* 69:278–279
21. Couteau E, Hernadi K, Seo JW, Thien-Nga L, Mikó C, Gaal R, Forro L (2003) CVD synthesis of high-purity multiwalled carbon nanotubes using CaCO₃ catalyst support for large-scale production. *Chem Phys Lett* 378:9–17
22. Wang Y, Gupta S, Nemanich R, Liu Z, Qin L (2005) Hollow to bamboolike internal structure transition observed in carbon nanotube films. *J Appl Phys* 98:014312 (1–6)
23. Grobert N (2007) Carbon nanotubes-becoming clean. *Mater Today* 10:28–35
24. Abbasi E, Aval SF, Akbarzadeh A, Milani M, Nasrabadi HT, Joo SW, Hanifehpour Y, Koshki KN, Asl RP (2014) Dendrimers: synthesis, applications, and properties. *Nanoscale Res Lett* 9:247–255
25. Yacaman MJ, Yoshida MM, Rendon L, Santiesteban JG (1993) Catalytic growth of carbon microtubules with fullerene structure. *Appl Phys Lett* 62:202–204
26. Mora E, Pigos JM, Ding F, Jakobson BI, Harutyunyan AR (2008) Low-temperature single-wall carbon nanotubes synthesis: feedstock decomposition limited growth. *J Am Chem Soc* 130:11840–11841
27. Nessim GD, Seita M, O'Brien KP, Hart AJ, Bonaparte RK, Mitchell RR, Thompson CV (2009) Low temperature synthesis of vertically aligned carbon nanotubes with electrical contact to metallic substrates enabled by thermal decomposition of the carbon feedstock. *Nano Lett* 9:3398–3405
28. Xiao Y, Ahmed Z, Ma Z, Zhou C, Zhang L, Chan M (2019) Low temperature synthesis of high-density carbon nanotubes on insulating substrate. *Nanomaterials* 9:473–482
29. Nessim GD (2010) Properties, synthesis, and growth mechanisms of carbon nanotubes with special focus on thermal chemical vapor deposition. *Nanoscale* 2:1306–1323
30. Tessonnier J, Su DS (2011) Recent progress on the growth mechanism of carbon nanotubes: a review. *Chemsuschem* 4:824–847
31. Dupuis A (2005) The catalyst in the CCVD of carbon nanotubes—a review. *Prog Mater Sci* 50:929–961
32. Jourdain V, Bichara C (2013) Current understanding of the growth of carbon nanotubes in catalytic chemical vapor deposition. *Carbon* 58:2–39
33. Hussein MZ, Jaafar AM, Yahaya AH, Masarudin MJ, Zainal Z (2014) Formation and yield of multi-walled carbon nanotubes synthesized via chemical vapour deposition routes using different metal-based catalysts of FeCoNiAl, CoNiAl and FeNiAl-LDH. *Int J Mol Sci* 15:20254–20265
34. Nagaraju N, Fonseca A, Konya Z, Nagy JB (2002) Alumina and silica supported metal catalysts for the production of carbon nanotubes. *J Mol Catal A: Chem* 181:57–62
35. Seo JW, Hernadi K, Miko C, Forro L (2004) Behavior of transition metals catalysts over laser-treated vanadium support surfaces in the decomposition of acetylene. *Appl Catal A* 260:87–91
36. Lee CJ, Park J, Yu JA (2002) Catalyst effect on carbon nanotubes synthesized by thermal chemical vapor deposition. *Chem Phys Lett* 360:250–255
37. Nath A, Shah A, Singh LR, Mahato M (2021) Waste plastic-derived NiO-MWCNT composite as visible light photocatalyst for degradation of methylene blue dye. *Nanotechnol Environ Eng* 6 (3):1–14

38. Senapati S, Shah A, Patra PK, Mahato M (2021) Measurement of elastic modulus of CNT composites: a nondestructive study. In: Fullerenes, nanotubes and carbon nanostructures 30:290–296
39. Samuel J, Shah A, Kumar D, Singh LR, Mahato M (2021) Preparation, characterization and some electrochemical study of waste derived iron Oxide–Carbon nanocomposite. *Mater Today: Proc* 47:1048–1053
40. Das HJ, Shah A, Singh LR, Mahato M (2021) Waste derived low cost PbO–Carbon nanocomposite and its energy storage application. *Mater Today: Proc* 47:1072–1077
41. Schneider JJ, Maksimova NI, Engstler J, Joshi R, Schierholz R, Feile R (2008) Catalyst free growth of a carbon nanotube–alumina composite structure. *Inorg Chim Acta* 361:1770–1778
42. Hussain A, Liao Y, Zhang Q, Ding E, Laiho P, Ahmad S, Wei N, Tian Y, Jianga H, Kauppinen E (2018) Floating catalyst CVD synthesis of single walled carbon nanotubes from ethylene for high performance transparent electrodes. *Nanoscale* 10:9752–9759
43. Zhu HW, Xu CL, Wu DH, Wie BQ, Vajtai R, Ajayan PM (2002) Direct synthesis of long single-walled carbon nanotube strands. *Science* 6:884–886
44. Cheng HM, Li F, Su G, Pan HY, He LL, Sun X (1998) Large-scale and low-cost synthesis of single-walled carbon nanotubes by the catalytic pyrolysis of hydrocarbons. *Appl Phys Lett* 72:3282–3284
45. Radhakrishnan JK, Pandian PS, Padaki VC, Bhusan H, Rao KUB, Xie J, Abraham JK, Varadan VK (2009) Growth of multiwalled carbon nanotube arrays by chemical vapor deposition over iron catalyst and the effect of growth parameters. *Appl Surf Sci* 255:6325–6334
46. Mohammed IA, Bankole MT, Abdulkareem AS, Ochigbo SS, Afolabi AS, Abubakre OK (2017) Full factorial design approach to carbon nanotubes synthesis by CVD method in argon environment. *S Afr J Chem Eng* 24:17–42
47. Liu J, Jiang Z, Yu H, Tang T (2011) Catalytic pyrolysis of polypropylene to synthesize carbon nanotubes and hydrogen through a two-stage process. *Polym Degrad Stab* 96:1711–1719
48. Li Y, Zhang X, Tao X (2004) Growth mechanism of multiwalled carbon nanotubes with or without bundles by catalytic deposition of methane on Mo/MgO. *Chem Phys Lett* 386:105–110
49. Venkatesan S, Visvalingam B, Mannathusamy G, Viswanathan V, Rao AG (2018) Effect of chemical vapor deposition parameters on the diameter of multi-walled carbon nanotubes. *Int Nano Lett* 8:297–308
50. Shah KA, Najjar FA, Sharda T, Sreenivas K (2018) Synthesis of multi-walled carbon nanotubes by thermal CVD technique on Pt–W–MgO catalyst. *J Taibah Univ Sci* 12:230–234
51. Shukrullah S, Mohamed NM, Khan Y, Naz MY, Ghaffar A, Ahmad I (2017) Effect of gas flow rate on nucleation mechanism of MWCNTs for a compound catalyst. *J Nanomater* 2017:1–9
52. Bone WA, Coward HF (1908) The thermal decomposition of hydrocarbons. *J Chem Soc Trans* 93:1197–1225
53. Li Z, Chen J, Zhang X, Li Y, Fung KK (2002) Catalytic synthesized carbon nanostructures from methane using nanocrystalline Ni. *Carbon* 40:409–415
54. Gulino G, Vieira R, Amadou J, Nguyen P, Ledoux MJ, Galvagno S, Centi G, Huu C (2005) C₂H₆ as an active carbon source for a large-scale synthesis of carbon nanotubes by chemical vapor deposition. *Appl Catal A* 279:89–97
55. Zhou Z, Ci L, Chen X, Tang D, Yan X, Liu D (2003) Producing cleaner double-walled carbon nanotubes in a floating catalyst system. *Carbon* 41:2607–2611
56. Li Q, Yan H, Zhang J, Liu Z (2004) Effect of hydrocarbons precursors on the formation of carbon nanotubes in chemical vapor deposition. *Carbon* 42:829–835
57. Das N, Dalai A, Mohammadzadeh JSS, Adjaye J (2006) The effect of feedstock and process conditions on the synthesis of high purity CNTs from aromatic hydrocarbons. *Carbon* 44:2236–2245
58. Demirbas A (2004) Pyrolysis of municipal plastic wastes for recovery of gasoline-range hydrocarbons. *J Anal Appl Pyrolysis* 72:97–102
59. Encinar JM, González JF (2008) Pyrolysis of synthetic polymers and plastic wastes. Kinetic study. *Fuel Process Technol* 89:678–686

60. Wu C, Nahil MA, Miskolczi N, Huang J, Williams PT (2014) Processing real-world waste plastics by pyrolysis-reforming for hydrogen and high-value carbon nanotubes. *Environ Sci Technol* 48:819–826
61. Rodiles X, Reguero V, Vila M, Alemán B, Arévalo L, Fresno F, Shea VA, Vilatela JJ (2019) Carbon nanotube synthesis and spinning as macroscopic fibers assisted by the ceramic reactor tube. *Sci Rep* 9:9239–9249
62. Sengupta J (2018) Handbook of nanomaterials for industrial applications. In: *Micro and nano technologies*. Elsevier, Netherlands
63. Maghrebi M, Khodadadi AA, Mortazavi Y, Mhaisalkar S (2009) Detailed profiling of CNTs arrays along the growth window in a floating catalyst reactor. *Appl Surf Sci* 255:7243–7250
64. Masouleh LS, Mostoufi N, Khodadadi A, Mortazavi Y, Maghrebi M (2012) Modeling the growth of carbon nanotubes in a floating catalyst reactor. *Ind Eng Chem Res* 51:1143–1149
65. Venkataraman A, Amadi EV, Chen Y, Papadopoulos C (2019) Carbon nanotube assembly and integration for applications. *Nanoscale Res Lett* 14:220–267
66. Gohier A, Ewels CP, Minea TM, Djouadi MA (2008) Carbon nanotube growth mechanism switches from tip-to base-growth with decreasing catalyst particle size. *Carbon* 46:1331–1338